Protomeric Equilibria in the Ground and Excited States of 2-Pyridone. A Semiempirical Study Including Solvent Effects

Carlo Adamo,[a] Vincenzo Barone,*[,a] Sandrine Loison[a] and Camilla Minichino[b]
[a] *Dipartimento di Chimica, Università Federico II, via Mezzocannone 4, I-80134 Napoli, Italy*
[b] *Dipartimento di Chimica, Università della Basilicata, via Nazario Sauro 85, I-85100 Potenza, Italy*

Interconversion between lactim and lactam forms of 2-pyridone has been investigated for the ground and first excited electronic states by the AM1 semiempirical method. Only non-dissociative processes have been considered, namely direct intramolecular transfer, interconversion within a self-associated dimer, and a mechanism assisted by one water molecule. The role of bulk solvent has also been investigated by means of the polarizable continuum model. The results for the ground electronic state are generally comparable with those obtained by refined *ab initio* computations, except for a significant overestimation of energy barriers to intermolecular proton transfer. The results for the first excited electronic state are very similar, thus ruling out any interpretation of spectral shifts in terms of excited state proton transfer. The strong Stokes shift observed in fluorescence spectra can rather be ascribed to the significant skeletal modifications connected to electronic excitation. A nice correspondence has been found between structural characteristics and composition of frontier orbitals.

Protomeric (especially lactim–lactam) equilibria in hetero-aromatic compounds are involved in a number of biological processes, such as mutagenesis.[1,2] One of the simplest reactions, which can be considered as a prototype for tautomerism in nucleic acid bases, involves the system 2-pyridone/2-hydroxy-pyridine (2Py/2Hy). Several experimental studies have therefore been devoted to the problem of the relative stability of the two tautomers.[3–6] The main conclusion is that the lactim species is favoured in the gas phase or in non-polar solvents, while the lactam form predominates in aqueous solution or, more generally, in polar solvents.[4] Thus significant variations of the equilibrium constant are connected to self-association of the lactam form and to the greater stability of solvent–lactam complexes.[7] The results are supported by a number of theoretical studies.[8–14]

More recently, attention has shifted to the detailed mechanism of proton transfer (PT). In analogy with other systems,[15,16] two classes of PT reactions are, in principle, possible: (i) dissociative transfer, typical of acid–base reactions, *i.e.* stepwise protonation and deprotonation of the substrate. An example is the PT reaction in the related molecule 4-hydroxypyridine. In this case, in fact, intramolecular PT is forbidden by the long distance between donor and acceptor sites. Tautomerization can only take place by a solvent-mediated mechanism in which one solvent molecule accepts the proton from the donor site and another one gives a different proton to the acceptor site;[17] (ii) non-dissociative transfer, which is important in the gas phase, in aprotic media, and in neutral aqueous solution.

In turn, this latter mechanism, can be divided into three subclasses (see Fig. 1): (i) Direct PT between two sites of the molecule; (ii) Dimeric PT, in which interconversion occurs within a self-associated dimer; (iii) Assisted PT, in which one or two amphiprotic molecules are also directly involved in the process. Experimental studies[18] have shown that this process is the most important in aqueous solution.

Non-dissociative PT has been extensively studied by quantum-mechanical methods. In particular Field and Hillier[10] investigated all three possible mechanisms in the gas phase. Owing to the large energy barrier obtained in all the quantum-mechanical computations,[10,12,13,19] direct PT seems unlikely. Moreover, the energetics of dimeric and assisted PT are very similar, so that computations concerning the latter (which occurs in a smaller system) are also representative for the former. Modulation effects induced by the solvent have been taken into account in two recent studies,[13,19] devoted to the bare molecules 2Hy and 2Py. No attempt has been made to extend this treatment to kinetic aspects, nor to investigate excited electronic states. These features may be significant since several molecules having nearby proton donor and acceptor sites undergo protomeric shifts in some excited electronic state (the so called Excited State Proton Transfer, ESPT, process). The signature of this process is a strong Stokes red-shifted fluorescence emission following absorption of a UV photon. Several spectroscopic studies have therefore been undertaken in this connection.[7,20–26] In particular Kuzuya and co-workers[20] have found that the absorption spectrum of 2Py in cyclohexane solution is characterized by two bands, at 268 and 300 nm, corresponding to lactim and lactam forms, respectively. Two bands are also present in the emission spectrum, but red-shifted

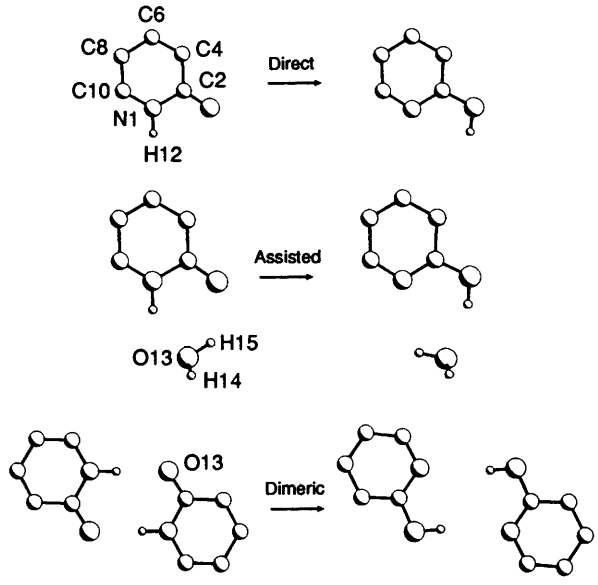

Fig. 1 Various types of non-dissociative proton transfers for 2-pyridone

to 303 and 367 nm.[20] The red-shift of the higher wavelength band from 300 to 367 nm is similar to that occurring in other systems where ESPT is operative.[16] The role of the solvent can be analysed by comparing the above results to some very accurate absorption and emission spectra recently reported for the 2Py/2Hy system in the gas phase.[21,25,26] In this case three bands are observed, centred at 334, 335 and 276 nm, respectively. The two higher wavelength bands were assigned to separate, non-planar conformers of the lactam.[21] The lower wavelength band was assigned to the lactim. A fourth band, at 325 nm, is characteristic of the 2-Py dimer.[26] No clear evidence has been found so far for an ESPT mechanism, but the problem is still open, as pointed out recently by Adamowicz and co-workers.[22]

In an attempt to gain further insight on the above points we have investigated, using semiempirical techniques, the possibility of tautomerization ruled by a non-dissociative PT mechanism, both in the ground and excited electronic states, and its relationship with the UV spectrum. We have also considered the role of bulk solvent in determining the stability of the two tautomeric forms, as well as its influence on the spectrum and on the PT energetics. We have, finally, investigated whether other structural deformations (*e.g.* skeletal ones) could be responsible for the observed spectral shifts.

Computational Details

All the computations have been carried out at the AM1 level[27] using the MOPAC 6.0 package.[28] Ground state geometries have been fully optimized at the Hartree–Fock (HF) level with the only constraint, based on previous *ab initio* results,[10] of planarity. The molecular geometry of the lowest excited singlet state was optimized with the same constraint using a minimal Configuration Interaction (CI), including the ground state and the configurations obtained by exciting one or two electrons from HOMO to LUMO. Using these geometries, transition energies were computed taking into account the 100 lowest energy configurations, obtained by exciting one or two electrons from the highest three occupied to the lowest two empty molecular orbitals.[29] To verify the quality of the transition energies computed at the AM1 level, we have also carried out some computations using the CNDO/S method,[30] which is *ad hoc* parametrized to obtain spectral parameters very close to experimental values. The role of bulk solvent has been investigated in the framework of the Polarizable Continuum Model (PCM).[31] In this model the overall change of the Gibbs free energy of solvation, ΔG_{solv}, is the sum of three terms [eqn. (1)]. The dispersion–repulsion term $\Delta G_{disp-rep}$ is evaluated by

$$\Delta G_{solv} = \Delta G_{el} + \Delta G_{disp-rep} + \Delta G_{cav} \quad (1)$$

means of empirical two-body potentials and assuming simple step forms for solute–solvent pair correlation functions.[32] The cavitation contribution ΔG_{cav} is computed in terms of the Scaled Particle Theory.[33] Both terms depend on the cavity surface, which is also involved in the electrostatic contribution. In fact, a charge distribution arises in each point of the cavity surface from the combined effect of the electric fields generated by the polarized solute (ζ_ρ) and the residual charge distribution on the surface (ζ_σ) given by eqn. (2) where the subscript n_- indicates a

$$\sigma(s) = -\frac{\varepsilon - 1}{4\pi\varepsilon}\left[\zeta_\rho(s) + \zeta_\sigma(s)\right]_{n_-} \quad (2)$$

limiting value on the concave side of the surface. The continuous charge distribution $\sigma(s)$ can be replaced by a set of discrete point charges. To this end, the surface S of the cavity is divided into portions ΔS, small enough that $\sigma(s)$ can be considered constant at their interiors. From a practical point of view, the cavity is represented by interlocking spheres centred on (all or part of) the atoms of the solute. The surface of each sphere is, in turn, divided into a predefined number of finite elements (usually triangles), whose centres, surfaces and orientations provide all the necessary information to set up the computations.[34] The evaluation of $\sigma(s)$ at the centre of each finite element can be done *via* eqn. (2), but the dependence of the electric field on $\sigma(s)$ demands an iterative procedure. This latter can be divided into the following steps.

(1) An initial set of surface charge densities σ^0 (and of corresponding point charges) is originated by the electric field generated by the unperturbed solute [eqns. (3a) and (3b)].

$$\sigma^0(s) = -\frac{\varepsilon - 1}{4\pi\varepsilon}\zeta^0{}_\rho(s)_{n_-} \quad (3a)$$

$$q^0 = \sigma^0(s)\Delta S \quad (3b)$$

(2) The charges at the centre of the surface elements generate an additional contribution $\zeta^0{}_\sigma$ to the electric field. The charge density is improved by substituting in eqn. (3) the overall electric field [eqn. (4)].

$$\sigma^1(s) = -\frac{\varepsilon - 1}{4\pi\varepsilon}(\zeta^0{}_\rho + \zeta^0{}_\sigma)_{n_-} \quad (4a)$$

$$q^1 = \sigma^1(s)\Delta S \quad (4b)$$

This new charge distribution generates, in turn, a modified electric field $\zeta^1{}_\sigma$, which, introduced into eqn. (4) leads to charges q^2, and so on, up to convergence to a final set of charges q^f.

(3) The electric field arising from the point charges q^f, is added to the Hamiltonian of the solute, leading to a new charge distribution $\rho^1(r)$.

(4) Steps (2) and (3) are iterated until self consistency is reached. The need to use a comparable procedure for different electronic states prompted us to avoid introduction of the reaction field in the solute hamiltonian [thus eliminating steps (3) and (4)] and to compute the electric field of the solute by means of its Mulliken atomic populations. Neither simplification should alter the general trends provided by a continuum solvent model.

Starting from the above quantities, we can compute solvent shifts on absorption and emission spectra, following a cyclic process.[35]

(a) The solute in the ground electronic state is in equilibrium with the solvent. The solute charge distribution ρ_{gs} gives rise to a surface charge distribution σ, which can be divided into an orientational and an inductive component. The total surface charge and the inductive component are formally given by the same expression [eqn. (2)]. However the relative permittivity entering the equation is the static relative permittivity ε in the former case, and ε_∞ (the square of optical refractive index extrapolated to infinite wavelength) in the latter. The orientational contribution is then obtained as a difference [eqn. (5)].

$$\sigma_a(\rho_{gs}, \varepsilon) = \sigma_{ind}(\rho_{gs}, \varepsilon_\infty) + \sigma_{or} \quad (5)$$

(b) The solute absorbs a photon and reaches the excited state, characterized by a new charge distribution, ρ_{ex}. Since the electronic transition time is much shorter than the orientational relaxation time, the solvent experiences the changes in ρ uniquely through its inductive part, so the new σ can be expressed as eqn. (6). From steps (a) and (b) we can compute

Table 1 Bond lengths (Å) and valence angles (degrees) of 2Hy and 2Py in the S_0 and S_1 electronic states

Atoms	2Py(S_0)	TS(S_0)	2Hy(S_0)	2Py(S_1)	TS(S_1)	2Hy(S_1)
N1–C2	1.41	1.39	1.36	1.45	1.43	1.35
C2–O3	1.25	1.31	1.38	1.25	1.30	1.35
C2–C4	1.46	1.41	1.42	1.41	1.39	1.48
C4–C6	1.36	1.39	1.39	1.42	1.43	1.39
C6–C8	1.43	1.41	1.40	1.37	1.39	1.38
C8–C10	1.37	1.40	1.40	1.45	1.43	1.46
N1–H12	0.99	1.36	2.39	0.99	1.39	2.42
H12–O3	2.48	1.43	0.97	2.46	1.36	0.97
N1–C2–O3	118.1	101.3	119.9	114.9	98.9	121.6
N1–C2–C4	116.6	122.5	124.1	116.9	123.8	124.9
C2–C4–C5	115.6	120.3	119.9	117.3	121.4	119.2
C2–C4–C6	120.9	116.4	117.5	122.1	117.2	116.0
C4–C6–C7	121.2	119.7	120.1	118.7	119.3	119.1
C4–C6–C8	120.2	121.1	119.5	119.8	119.1	120.4
C6–C8–C9	120.1	120.4	121.1	123.8	120.9	122.7
C2–N1–C10	121.3	120.2	116.4	120.3	117.7	116.5

$$\sigma_b = \sigma_{ind}(\rho_{ex}, \varepsilon_\infty) + \sigma_{or} \quad (6)$$

solvent-induced shifts in absorption spectra.

(c) After a sufficiently long time, the solvent rearranges around the excited solute molecule and eqn. (7) holds.

$$\sigma_c(\rho_{ex}, \varepsilon) = \sigma_{ind}(\rho_{ex}, \varepsilon_\infty) + \sigma'_{or} \quad (7)$$

(d) The solute emits a photon and again reaches the ground state. As before, during this process only the inductive part of σ is changed [eqn. (8)]. From steps (c) and (d) we can evaluate

$$\sigma_d = \sigma_{ind}(\rho_{gs}, \varepsilon_\infty) + \sigma'_{or} \quad (8)$$

solvent-induced shifts in fluorescence spectra.

(e) The equilibrium between solute and solvent is restored and the same physical situation as in step (a) is obtained.

We refer the reader to the original papers[31,35] for a deeper discussion of several more subtle aspects of the model, such as the shape of the cavity, the size of the surface elements, *etc.* Here we want only to point out that for apolar solvents (such as cyclohexane, considered in this study) the two relative permittivities, ε and ε_∞ are equal, so that the solvent induces identical spectral shifts in absorption and emission processes.

Results

The size of the systems and the need to investigate potential energy surfaces for excited electronic states, do not allow the use of sophisticated *ab initio* CI or multiconfigurational schemes. This holds especially if one considers that accurate *ab initio* computations of hydrogen bond energetics require large polarized basis sets[36,37] and BSSE corrections.[38] Having to resort to semiempirical methods, the reliability of the chosen procedure (here AM1) must be critically judged with special reference to systems and processes as close as possible to those to be investigated. According to a large number of published applications, the AM1 method yields reliable results for ground state geometries, heats of formation and relative stabilities of tautomeric species.[39] The quality of the AM1 approximation for excited states is more difficult to assess, since only a few papers have been published on this topic.[16,40–46] Encouraging results have been recently reported concerning the dynamics of some photochemical processes[41,42] and conformational changes induced in polyenes by photoexcitation.[43,44] In particular Ertl[45] has pointed out that AM1 yields geometrical parameters for excited states in good agreement with experiment, its only drawback being a slight underestimation of transition energies.[28] From another point of view, the AM1 method provides qualitatively correct hydrogen bond geometries and strengths, but generally overfavours bifurcated structures with respect to linear ones.[47] Test computations on malonaldehyde and literature data[47] suggest that the calculation of energy barriers to proton transfer can be significantly overestimated. General trends are, however, correctly reproduced, thus allowing the use of *ad hoc* scaling procedures (*vide infra*).

Proton Transfer Energetics.—We have investigated the ground electronic state (S_0) and the first excited singlet (S_1) of all the systems shown in Fig. 1, and the transition states (TS) connecting them. In all cases the S_1 state is essentially obtained by a π–π^* HOMO–LUMO excitation with very small contributions of other excitations, like HOMO–(LUMO + 1). The geometrical parameters for the S_0 and S_1 states of 2PY and 2Hy are collected in Table 1. Since intramolecular angles and distances of the other complexes are essentially the same as in the bare molecules, only intermolecular parameters are given in Table 2. It is noteworthy that electron excitation induces only small geometrical changes in lactim systems, whereas the whole conjugated ring is significantly distorted in lactam systems (see Table 2).

The energetics of PT in the S_0 and S_1 states are summarized in Table 3. As mentioned above, the AM1 results for the ground state are quite satisfactory, especially as regards the energy differences between the two tautomeric forms (the endothermicity of the tautomerization reaction). The computations at the CI level indicate 2Hy as the more stable molecule in the ground state and in the adduct with one water molecule (−4.6 kcal mol^{-1} and −1.6 kcal mol^{-1} with respect to 2Py).* The greater stability of the lactim form is in agreement with experimental findings and is reproduced by *ab initio* computations only using very large basis sets and massive correlation treatments.[12] The situation is reversed in the dimer, $(2Py)_2$ being more stable than $(2Hy)_2$ by about 7 kcal mol^{-1}. Addition of Zero Point Energies (ZPE) leads to a net stabilization of the 2Hy species and of the transition state structures with respect to the 2Py molecules. Note that ZPE computed using unscaled AM1 frequencies are very close to those obtained by scaled *ab initio* values (see Table 3).

The activation energy of the tautomerization reaction calculated for the monomer is very close to the *ab initio* results

* 1 cal = 4.184 J.

Table 2 Computed intermolecular distances (Å) and angles (degrees) of 2Hy/2Py complexes in the S_0 and S_1 electronic states

Atoms	2Py(S_0)	TS(S_0)	2Hy(S_0)	2Py(S_1)	TS(S_1)	2Hy(S_1)
Complex with H_2O						
N1–H12	1.00	1.57	2.65	1.00	2.52	2.65
H12–O13	2.11	1.12	0.96	2.10	1.05	0.96
N1–O13	2.97	2.50	3.19	2.98	2.51	3.15
O3–H15	2.12	1.47	0.98	2.14	1.41	0.98
O3–O13	2.86	2.39	3.02	2.87	2.38	2.98
O13–H15	2.11	1.09	2.06	0.97	1.11	2.02
N1–H12–O13	142.0	144.1	115.6	144.4	141.6	115.6
H12–O13–H15	91.0	101.3	49.2	93.4	100.9	98.7
O13–H15–O3	132.5	137.4	165.5	129.0	141.6	163.1
H15–O13–H14	103.6	106.9	113.1	103.7	106.9	119.6
Dimer						
N1–H12	1.04		2.60	1.00		2.43
H12–O13	2.03		0.97	2.06		0.98
N1–O13	3.04		3.57	3.07		3.60
N1–H12–O13	176.7		173.5	175.8		173.3

Table 3 Endothermicities (ΔE) and activation energies ($\Delta E^{\ddagger}$) for the tautomerization of 2-pyridone in the gas phase. Energy values (in kcal mol^{-1}) refer to fully optimized geometries and the subscripts indicate direct (2Py/2Hy), assisted (2Py-H_2O/Hy-H_2O) and dimeric ($2Py_2/2Hy_2$) models of non-dissociative PT. *Ab initio* results are from ref. 10

	AM1 ground state			*Ab initio* ground state			AM1 excit. state	
	HF	CI	CI + ZPE	HF	CI	CI + ZPE	CI	CI + ZPE
ΔE_{dir}	−0.5	−4.6	−5.3	1.7	3.4	2.6	15.7	17.7
$\Delta E^{\ddagger}_{dir}$	54.1	52.1	48.5	50.9	43.7	40.1	58.4	54.4
ΔE_{ass}	2.2	−1.6	−2.3	2.9	3.1	2.4	19.6	21.3
$\Delta E^{\ddagger}_{ass}$	43.5	41.7	37.4	15.8	12.9	8.6	48.7	46.5
ΔE_{dim}	7.1	6.9	4.9	9.6	8.4		24.6	25.5

Table 4 Absorption spectral maxima (in nm) of the 2Py/2Hy systems in the gas phase and in cyclohexane solution

	Computed			Experimental	
Molecule	AM1	CNDO/S	AM1/PCM	Gas phase[a]	Solution[b]
Py	311	302	307	334/335	300
Hy	281	273	282	276	268
Py (H_2O)	311	302		328	
Hy (H_2O)	282	273		282	
$(Py)_2$	305	291	300	325[c]	
$(Hy)_2$	258	271	357		

[a] Ref. 23. [b] Ref. 21. [c] Ref. 26. [d] Ref. 20.

and its very high value rules out a direct PT mechanism. On the other hand, AM1 activation energies are overestimated by about 100% with respect to *ab initio* results for the adduct with one water molecule and for the dimer. Use of *ab initio* values, or scaling of AM1 ones, gives, anyway, values too high to consider further any kind of non-dissociative PT in the ground electronic state. In the S_1 electronic state the lactam form is significantly stabilized; for instance 2Py is more stable than 2Hy by 16 kcal mol^{-1} and $(2Py)_2$ more stable than $(2Hy)_2$ by 25 kcal mol^{-1}. Other general trends are essentially identical in S_1 and S_0 electronic states, especially concerning the energy barriers to dimeric and assisted PTs. The similarity of activation barriers in the two electronic states is confirmed by preliminary *ab initio* computations.[48] Thus a simple scaling of AM1 results could produce reliable values also for activation energies. Inclusion of solvent (cyclohexane in the present case) effects do not alter general trends. More precisely, non-electrostatic contributions are nearly the same for lactim, lactam and TS, whereas the electrostatic term favours the form with the largest dipole moment. This last effect is, however, quite small due to the low relative permittivity of cyclohexane.

In summary, the possibility of direct PT is ruled out both the the S_0 and S_1 electronic states. On the other hand, dimeric and assisted mechanisms for ESPT deserve further investigation, especially concerning the S_1 state.[48] A different structural origin needs to be found to explain the red shift observed in the fluorescence spectra of 2Py.

Electronic States and UV Spectra.—The transition energies computed for the absorption spectra of the different systems are reported in Table 4. Energy values refer to vertical transitions, starting from the optimized geometries of the ground states. Transition energies are in fairly good agreement with experiment. As mentioned in the introduction, the UV absorption spectrum of 2Py in cyclohexane shows a strong band around 300 nm, while the spectrum of 2Hy has one band centred at 268

Table 5 Dipole moments (μ in Debyes) and different contributions (kcal mol^{-1}) to solvation free energies. Energy values are computed using AM1 optimized geometries and charges, while dipole moments are computed at the *ab initio* level using a STO-3G basis set

	Ground electronic state			Excited electronic state		
Parameter	Py	TS	Hy	Py	TS	Hy
μ_{gas}	3.12	2.48	1.09	1.30	2.47	1.09
μ_{sol}	3.32	2.65	1.16	1.53	2.66	1.58
ΔG_{el}	−5.11	−5.17	−3.03	−4.21	−3.66	−3.61
ΔG_{cav}	6.60	6.38	6.57	6.62	6.40	6.54
$\Delta G_{disp-rep}$	−10.13	−10.48	−10.41	−10.16	−10.42	−10.35

Table 6 Spectral maxima (in nm) in the fluorescence spectra of the system 2Py/2Hy in the gas phase and in cyclohexane solution

Molecule	AM1	CNDO/S	AM1/PCM	Exp.[a]
Py	370	351	368	367
Hy	286	280	289	303
Py (H_2O)	368	349		
Hy (H_2O)	288	281		
$(Py)_2$	366	335	366	
$(Hy)_2$	259	278	261	

[a] Ref. 20.

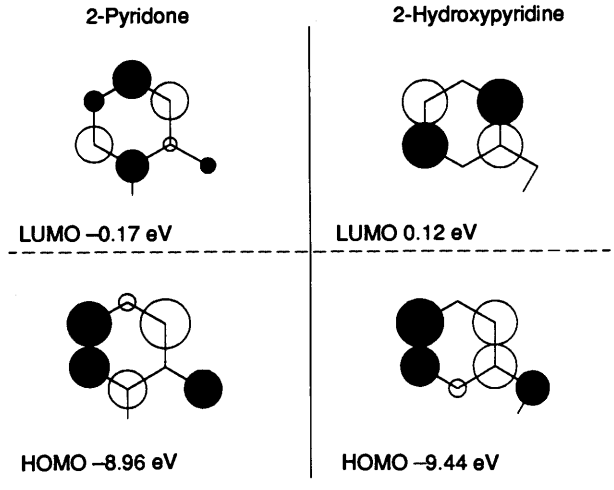

Fig. 2 Composition of frontier orbitals in 2-pyridone and 2-hydroxypyridine

nm.[20] The Time of Flight Mass Spectroscopy (TOFMS) results are also reported for the bare molecules (334/335 and 276 nm), for the clusters with one water molecule (328 and 282 nm), and for the 2Py dimer (325 nm).[26] The computed AM1 transition energies of 2Py and 2Hy *in vacuo* are at 311 and 281 nm respectively, shifting to 305 and 258 nm in the case of the symmetric dimer molecules. The CNDO/S results are in fair agreement with AM1 ones (see Table 4).

AM1 geometries and charges have been used to compute spectral shifts in cyclohexane in the framework of the PCM. In Tables 4 and 5 we report the overall solvent effect on absorption transitions and the partial (*i.e.* electrostatic, cavitation and dispersion–repulsion) contributions, respectively. Spectral shifts induced by the solvent are quite small, but improve, in each case, agreement between theory and experiment.

The two TOFMS transitions for 2Py at 334 and 335 nm were assigned by Nimlos *et al.*[21] to two different non-planar geometries arising from different pyramidal environments of the nitrogen atom. This analysis was recently confirmed by Held *et al.*[25] on the basis of a very accurate analysis of experimental results, supported by a sophisticated theoretical model. We investigated briefly this point, computing the transition energy for different positions of the nitrogen atom out of the molecular plane. In particular for an out-of-plane angle of 20° the computed transition is at 340 nm, very close to experimental results. However, this structure lies about 14 kcal mol^{-1} above the planar one. Since *ab initio* results confirm the planarity of the ground state of 2Py,[10] the doubling of the band around 334 nm should probably be ascribed to a different effect. In Table 6 we show the computed transition energies for the fluorescence spectra. The energies refer to vertical transitions from the optimized geometries of the first excited singlet state. In this case also the agreement between computed and experimental results is generally good.

The emission wavelengths of 2Py and 2Hy are red-shifted with respect to the corresponding absorption wavelengths. This shift is more evident in 2Py (from 300 to 367 nm), than in 2Hy (from 268 to 303 nm). This behaviour is generally interpreted in terms of direct intramolecular proton transfer in the excited electronic state.[15] In the case of the system 2Hy/2Py this effect is, instead, connected to strong deformations of bond distances in the aromatic ring upon electronic excitation (see Tables 1 and 2). In the 2Py molecule, the changes involve all the bonds of the ring, the most important being the increase of C8–C10 (1.37/1.45 Å) and of C4–C6 (1.36/1.42 Å) distances and the decrease of C6–C8 (1.43/1.37 Å) bond lengths. For the 2Hy molecule the changes are less dramatic, involving only C2–C4 (from 1.42 to 1.48 Å) and C8–C10 (from 1.40 to 1.46 Å) bonds.

The electronic origin of these effects is quite apparent on inspection of the composition of the frontier orbitals of 2Py and 2Hy sketched in Fig. 2. The HOMOs of the two tautomers are very similar to one another. They mainly correspond to bonding contributions of the 2pπ atomic orbital of N1, C2 and C4 and of C8 and C10, with an antibonding interaction with the 2pπ orbital of the oxygen atom. The HOMO energy of 2Hy is lower by about 0.5 eV, due to a stronger N1–C2–C4 bonding interaction. The LUMOs are dominated by antibonding interactions. However small bonding C6–C8 and C2–C4 interactions are only operative in 2Py; these lower the LUMO energy of the lactam form by about 0.3 eV *versus* that of the lactim form. These effects explain the stabilization of 2Py with respect to 2Hy upon electron excitation from S_0 to S_1. Furthermore, the large red shift (about 60 nm at the AM1 level) between the absorption and fluorescence spectra of 2Py is strongly related to the very different structure of the HOMO and LUMO orbitals. This difference is reflected in the molecular geometry and in the vibrational frequencies. This simple scheme is further supported by considerations based on the computed bond orders and net atomic charges. The most important changes produced in the 2Py molecule by excitation are the significant decreases in the bond orders of the C8–C10 and C4–C6 double bonds (1.65/1.12 and 1.72/1.15, respectively), and the corresponding increase of the C6–C8 single bond (1.16/1.54). Comparatively smaller modifications occur in the 2Hy molecule, the largest change (from 1.31 to 0.93) involving the C2–C4 bond order.

Conclusions

In this paper we have reported the results of a comprehensive analysis of the lactim–lactam equilibrium of 2-pyridone in both the ground and first excited electronic states. This study points out a number of crucial aspects connected to the description of spectroscopic and/or reactive processes in solution. As a first point, last generation solvent models, taking into account solute polarization and quantum effects, allow the description of feedback effects, which could be of paramount importance, especially for processes involving severe electron density redistribution in polar solvents. It has next been shown that both the kinetics and thermodynamics of protomeric equilibria can be significantly modified by the direct involvement of a single solvent molecule. The further modulation induced by bulk solvent is comparatively smaller, but, sometimes, non-negligible. From another point of view, structural interpretations of spectroscopic results require great care, since different modifications (here skeletal *vs.* hydrogen bridges) can sometimes lead to similar results (here red shift of fluorescence).

From a more general point of view, the most significant outcome of this and related studies is that a semiquantitative description of spectroscopic and reactive processes of large molecules in solution is becoming more and more feasible thanks to the development of very efficient quantum-mechanical tools and the combined use of complementary methods. This offers the opportunity to start more systematic studies aimed at the recognition of general trends and rules of thumb for those mechanisms in large classes of related systems.

Acknowledgements

The authors acknowledge the Italian Research Council (*comitato Informatica*) for financial support.

References

1 J. S. Kwiatkowski, T. J. Zielinski and R. Rein, *Adv. Quantum Chem.*, 1986, **18**, 85.
2 M. D. Topal and J. R. Fresco, *Nature*, 1976, **263**, 285; W. G. Cooper, *Int. J. Quantum Chem.*, 1978, **14**, 71.
3 P. Beak, J. B. Covington and S. G. Smith, *J. Am. Chem. Soc.*, 1976, **98**, 186.
4 P. Beak, *Acc. Chem. Res.*, 1977, **10**, 186 and refs. therein.
5 S. Suradi, N. El Saiad, G. Pilcher and H. A. Skinner, *J. Chem. Thermodyn.*, 1982, **14**, 45.
6 P. Beak, J. B. Covington, S. G. Smith, J. M. White and J. M. Ziegler, *J. Org. Chem.*, 1980, **45**, 1354.
7 P. Beak, F. S. Fry, J. Lee and F. Steele, *J. Am. Chem. Soc.*, 1976, **98**, 171.
8 H. B. Schlegel, P. Gund and E. M. Fluder, *J. Am. Chem. Soc.*, 1982, **104**, 5347.
9 M. J. Scanlan and I. H. Hillier, *Chem. Phys. Lett.*, 1984, **107**, 330.
10 M. J. Field and I. H. Hillier, *J. Chem. Soc., Perkin Trans. 2*, 1987, 617.
11 L. Adamowicz, *Chem. Phys. Lett.*, 1989, **161**, 73.
12 M. Moreno and W. H. Miller, *Chem. Phys. Lett.*, 1990, **171**, 475.
13 M. W. Wong, K. B. Wiberg and M. J. Frisch, *J. Am. Chem. Soc.*, 1992, **114**, 1645.
14 Z. Slanina, A. Les and L. Adamowicz, *J. Mol. Struct. THEOCHEM*, 1992, **257**, 491.
15 See for example: P. F. Barbara, P. K. Walsh and L. E. Brus, *J. Phys. Chem.*, 1989, **93**, 29; T. Elsaesser and W. Kaiser, *Chem. Phys. Lett.*, 1986, **128**, 231; T. Nishiya, S. Yamauchi, N. Hirota, M. Baba and I. Hanazaki, *J. Phys. Chem.*, 1986, **90**, 5730; J. Goodman and L. E. Brus, *J. Am. Chem. Soc.*, 1978, **100**, 7472; N. P. Ernsting, *J. Phys. Chem.*, 1985, **89**, 4, 832; G. Smulevich and P. Foggi, *J. Chem. Phys.*, 1987, **87**, 5657.
16 A. Peluso, C. Adamo and G. Del Re, *J. Math. Chem.*, 1992, **10**, 249 and refs. therein.
17 P. Beak, J. B. Covington and J. M. White, *J. Org. Chem.*, 1980, **45**, 1347.
18 O. Bensaude, M. Chevrier and J. E. Dubois, *J. Am. Chem. Soc.*, 1979, **101**, 2423.
19 P. Cieplak, P. Bash, U. C. Singh and P. A. Kollman, *J. Am. Chem. Soc.*, 1987, **109**, 6283.
20 M. Kuzuya, A. Noguchi and T. Okuda, *J. Chem. Soc., Perkin Trans. 2*, 1985, 1423.
21 M. R. Nimlos, D. F. Kelley and E. R. Bernstein, *J. Phys. Chem.*, 1989, **93**, 643.
22 M. J. Nowak, L. Lapinski, J. Fulara, A. Les and L. Adamowicz, *J. Phys. Chem.*, 1992, **96**, 1562.
23 A. Fujimoto, K. Inuzuka and R. Shiba, *Bull. Chem. Soc. Jpn.*, 1981, **54**, 2801.
24 R. Tembreuil, C. H. Sin, H. M. Pang and D. M. Lubman, *Anal. Chem.*, 1985, **57**, 2911.
25 A. Held and D. W. Pratt, *J. Am. Chem. Soc.*, 1990, **112**, 8629.
26 A. Held, B. B. Champagne and D. W. Pratt, *J. Chem. Phys.*, 1991, **95**, 8732.
27 M. J. S. Dewar, E. G. Zoebisch, E. F. Healy and J. J. P. Stewart, *J. Am. Chem. Soc.*, 1985, **107**, 3902.
28 J. J. P. Stewart, *MOPAC 6.0*, Quantum Chemistry Program Exchange, program n. 455.
29 M. J. S. Dewar, M. A. Fox, K. A. Campbell, C. C. Chen, J. B. Friedheim, M. K. Halloway, S. C. Kim, P. B. Lieschesky, A. M. Pakiari, T. P. Tien and E. G. Zoebisch, *J. Comput. Chem.*, 1984, **5**, 480.
30 J. Del Bene and H. H. Jaffè, *J. Chem. Phys.*, 1968, **48**, 1807; J. Del Bene and H. H. Jaffè, *J. Chem. Phys.*, 1968, **49**, 1221.
31 S. Miertus, E. Scrocco and J. Tomasi, *Chem. Phys.*, 1981, **55**, 117; S. Miertus and J. Tomasi, *Chem. Phys.*, 1982, **65**, 239.
32 F. Floris and J. Tomasi, *J. Comput. Chem.*, 1989, **10**, 616.
33 R. A. Pierotti, *Chem. Rev.*, 1976, **76**, 717.
34 J. L. Pascual-Ahuir, E. Silla, J. Tomasi and R. Bonaccorsi, *J. Comput. Chem.*, 1987, **8**, 778; J. L. Pascual-Ahuir and E. Silla, *J. Comput. Chem.*, 1990, **11**, 1047; J. L. Pascual-Ahuir and E. Silla, *J. Comput. Chem.*, 1991, **12**, 1077.
35 R. Cimiraglia, S. Miertus and J. Tomasi, *Chem. Phys. Lett.*, 1981, **80**, 286; R. Bonaccorsi, R. Cimiraglia and J. Tomasi, *Chem. Phys. Lett.*, 1983, **99**, 77.
36 M. Seel M. and G. Del Re, *Int. J. Quantum Chem.*, 1986, **30**, 563.
37 P. Amodeo and V. Barone, *J. Am. Chem. Soc.*, in the press.
38 Z. Latajka, S. Scheiner and G. Chalasinski, *Chem. Phys. Lett.*, 1992, **196**, 384.
39 W. M. F. Fabian, *J. Comput. Chem.*, 1991, **12**, 17.
40 J. Troe and K. M. Weitzel, *J. Chem. Phys.*, 1988, **88**, 7030.
41 M. J. S. Dewar and C. Doubleday, *J. Am. Chem. Soc.*, 1978, **100**, 4935.
42 H. E. Zimmermann and A. M. Weber, *J. Am. Chem. Soc.*, 1989, **111**, 995.
43 C. Rulliere, A. Declemy, P. Kottis and L. Ducasse, *Chem. Phys. Lett.*, 1985, **117**, 583.
44 P. Ertl, *Int. J. Quantum Chem.*, 1990, **38**, 231; P. Ertl and J. Leska, *J. Mol. Struct. THEOCHEM*, 1988, **165**, 1.
45 P. Ertl, *Collect. Czech. Chem. Commun.*, 1990, **55**, 1399.
46 K. Das, N. Sarkar, D. Majumdar and K. Bhattacharya, *Chem. Phys. Lett.*, 1992, **198**, 443.
47 E. L. Coitino, K. Irving, J. Rama, A. Iglesias, M. Paulino and O. N. Ventura, *J. Mol. Struct. THEOCHEM*, 1990, **210**, 405.
48 C. Adamo, V. Barone and C. Minichino, unpublished results.

Paper 2/06019A
Received 11*th November* 1992
Accepted 5*th January* 1993